Trends in Renewable Energy
OPEN ACCESS ISSN:2376-2144
Peer-Reviewed Article futureenergysp.com/index.php/tre

# Business Analytics and IT in Smart Grid – Part 3: New Application Aspect and the Quantitative Mitigation Analysis of Piecewise Monotonic Data Approximations on the iSHM Class Map Footprints of Overhead Low-Voltage Broadband over Power Lines Topologies Contaminated by Measurement Differences

Athanasios G. Lazaropoulos[1,2,*]

*1: School of Electrical and Computer Engineering / National Technical University of Athens / 9 Iroon Polytechniou Street / Zografou, GR 15780*
*2: Department of Industrial Design and Production Engineering / School of Engineering / University of West Attica / 250 Thivon & P. Ralli / Athens, GR 12244*

Received March 25, 2020; Accepted May 4, 2020; Published May 14, 2020

Big data that overwhelm smart grid (SG) are susceptible to errors that can further affect business analytics and related human decisions. In [1], the impact of measurement differences that follow various distributions has been examined via initial Statistical Hybrid Model (iSHM) footprints while the mitigation impact of piecewise monotonic data approximations has been qualitatively assessed via corresponding iSHM footprints in [2]. In this companion paper, the potential of applying piecewise monotonic data approximations in the intrinsic procedure of iSHM rather than its inputs and the quantitative mitigation analysis of piecewise monotonic data approximations against measurement differences via iSHM footprints are proposed for the overhead low-voltage broadband over power lines (OV LV BPL) topologies.

*Keywords: Smart Grid; Broadband over Power Lines (BPL) networks; Power Line Communications (PLC); Distribution and Transmission Power Grids; Capacity, Statistics; Business Analytics; IT; Modeling*

**Corresponding author:* AGLazaropoulos@gmail.com

Tr Ren Energy, 2020, Vol.6, No.2, 214-233. doi: 10.17737/tre.2020.6.2.00119

## Nomenclature

| | |
|---|---|
| APDmd | Average Percent Distance computation of the Measurement Differences |
| APDna | Average Percent Distance computation of the New Aspect |
| APDta | Average Percent Distance computation of the Traditional Aspect |
| BPL | Broadband over Power Lines |
| BPMN | Business Process Model and Notation |
| CASD | Channel Attenuation Statistical Distribution |
| CUD | Continuous Uniform Distribution |
| DHM | deterministic hybrid model |
| EMI | ElectroMagnetic Interference |
| IP | Internet Protocol |
| IT | Information Technology |
| iSHM | initial Statistical Hybrid Model |
| LOS | Line-of-Sight |
| LV | Low Voltage |
| L1PMA | L1 Piecewise Monotonic Approximation |
| L2WPMA | L2 Weighted Piecewise Monotonic Approximation |
| MLE | Maximum Likelihood Estimator |
| MTL | Multiconductor Transmission Line |
| ND | Normal Distribution |
| OV | Overhead |
| SG | Smart Grid |
| TL | Transmission Line |
| WtG | Wire-to-Ground |

## 1. Introduction

BPL technology is among the communications proposals that are going to transform the vintage power grid into an advanced IP-based communications network enhanced with a plethora of broadband applications and business analytics, the so called SG [1]-[8]. The main advantage of SG is the reception of a plethora of data concerning the metering, monitoring and controlling of its infrastructure and equipment thus allowing the authorized personnel and customers to take decisions that further affect the SG operation. It is evident that right decisions urge reliable data and towards that direction piecewise monotonic data approximations contribute to the restoration of the contaminated data by measurement differences in OV LV BPL networks [1], [7], [9]-[11].

In this paper, it is already known that measurement differences are observed between the experimental and theoretical results during the transfer function determination of OV LV BPL topologies and are due to a number of practical reasons and "real-life" difficulties. Actually, coupling scheme transfer function determination occurs in the well-validated DHM that is the introductory core element of the recently proposed and here applied iSHM that is deployed for the statistical broadband channel description of OV LV BPL topologies [12]-[20]. Business analytics of SG exploit a plethora of related broadband iSHM tools, such as the definition procedure, the class maps and the iSHM footprints whose results are critically affected by the coupling scheme transfer function data of DHM. More specifically, it has been shown in [1] that the behavior of iSHM footprints due to the measurement differences of the OV LV BPL networks may be sensitive even to low intensities of measurement differences. In accordance with [1], when high measurement differences occur the broadband iSHM tools, such as the topology identification technique and the energy theft detection via iSHM footprint, can be totally jammed thus influencing the quality of business analytics of the SG and the supported human decisions. To enhance the reliability of SG data, piecewise monotonic data approximations, such as L1PMA and L2WPMA, have been deployed against the measurement differences while their qualitative evaluation was done via the respective L1PMA and L2WPMA iSHM footprints in [2]. Indeed, L1PMA and L2WPMA can achieve significant measurement difference restoration concerning the extent and the distance of iSHM footprints from the theoretical Weibull CASD MLEs of the real indicative OV LV BPL urban case A. Note that the qualitative methodology of [2] examined the degree of shrinkage and stress of the iSHM footprints due to measurement differences by the applied piecewise monotonic data approximations towards the theoretical Weibull CASD MLEs of the real indicative OV LV BPL urban case A.

In this paper, first, a new aspect concerning the location of the application of piecewise monotonic data approximations inside the iSHM operation flowchart is proposed. Until now, piecewise monotonic data approximations have been applied right after the application of DHM to the coupling scheme transfer function data of the examined OV LV BPL topologies in order to suppress the measurement difference contamination at that location [7], [9], [21]-[28]. Since the result of the multipath aggravation of OV LV BPL topologies can be treated as a superposition of spectral notches of various depths and extents onto the coupling scheme transfer function of the OV LV BPL "LOS" case [14], [17], [29], piecewise monotonic data approximations can alternatively focus on the output results of the coupling scheme channel attenuation

difference module Δ of iSHM that is anyway an internal iSHM procedure; the coupling scheme channel attenuation difference module Δ of iSHM gives as output the coupling scheme channel attenuation difference between each examined OV LV BPL topology and the OV LV BPL "LOS" case thus providing more uncorrelated data in comparison with the ones of the traditional aspect. The unbiased data of the coupling scheme channel attenuation difference module Δ of iSHM can be proven valuable for a more efficient application of piecewise monotonic data approximations under certain conditions [30]-[33].

Second, a quantitative methodology is proposed in this paper so that the assessment of the mitigation efficiency of piecewise monotonic data approximations against measurement differences can be feasible on the basis of the iSHM footprints of [2]. During the qualitative evaluation of L1PMA and L2WPMA in [2], it was clear that the critical intrinsic parameters of piecewise monotonic data approximations, such as L1PMA monotonic sections and L2WPMA sign changes, mainly affect the performance of piecewise monotonic data approximations against the measurement differences. The selection of the optimal numbers of L1PMA monotonic sections and L2WPMA sign changes has been made on the basis of the visual proximity of the respective L1PMA and L2WPMA iSHM footprints to the theoretical Weibull CASD MLEs for given real indicative OV LV BPL topology (say, real indicative OV LV BPL urban case A in [2]). Here, the evolution of the qualitative evaluation of the proximity is the proposal of a quantitative methodology that can compute the average distances of the piecewise monotonic data approximation iSHM footprints and iSHM footprints due to measurement differences and hence defines the critical intrinsic parameters of the piecewise monotonic data approximations by comparing and by sorting the gathered distances. Also, the new aspect, which is proposed in this paper, concerning the application of piecewise monotonic data approximations to the results of the coupling scheme channel attenuation difference module Δ of iSHM is also benchmarked through the new quantitative methodology.

The rest of this paper is organized as follows: Section II presents the mathematics of the new aspect regarding the application of piecewise monotonic data approximations to the results of the coupling scheme channel attenuation difference module Δ of iSHM. In Section III, the new quantitative methodology concerning the assessment of the mitigation efficiency of piecewise monotonic data approximations against measurement differences via iSHM footprints is presented. Section IV presents numerical results related with the application of the quantitative methodology and the new aspect of piecewise monotonic data approximation application location. Section V concludes this paper.

## 2. New Aspect of Application for the Piecewise Monotonic Data Approximations against Measurement Differences

With reference to the BPMN diagram of iSHM [34], iSHM consists of six Phases (*i.e.*, Phase A-F) while each Phase is clearly described by its procedure as well as its inputs and outputs. With reference to this BPMN diagram, Phase A consists of DHM that takes as inputs the examined real indicative OV LV BPL topology, the respective distribution MTL configuration and the applied coupling scheme while DHM results are the output of Phase A that is the theoretical coupling scheme transfer function

$H^{\mathrm{OVLV},C}(f_q)$, $q$=1,…,$Q$ when measurement differences are not assumed where $[\cdot]^C$ denotes the applied coupling scheme, $f_q$ is the flat-fading subchannel start frequency and $Q$ is the number of subchannels in the examined frequency range. When measurement differences are assumed during the preparation of iSHM footprints as in [1], [2], the measurement differences are treated as distributions; say, CUD of variable maximum value $a_{\mathrm{CUD}}$. After the measurement difference consideration, the output of Phase A, which is afterwards exploited by the iSHM footprints, is the measured coupling scheme transfer function that is given by [1], [5], [35]

$$\overline{H_{d1,d2,i}^{\mathrm{OVLV},C,D}}(f_q) = H^{\mathrm{OVLV},C}(f_q) + e_{d1,d2,i}^{D}(f_q),\ q=1,\ldots,Q,\ i=1,\ldots,I \tag{1}$$

where $[\cdot]^D$ denotes the applied measurement difference distribution –*i.e.*, CUD of this paper in accordance with [2]–, $d1$ is the first parameter of the applied measurement difference distribution (*i.e.*, the minimum value $-a_{\mathrm{CUD}}$ of CUD), $d2$ is the second parameter of the applied measurement difference distribution (*i.e.*, the maximum value $a_{\mathrm{CUD}}$ of CUD), $e_{d1,d2,i}^{D}(f_q)$ is the measurement difference at frequency $f_q$ for given measurement difference distribution and $I$ is the number of different $1 \times Q$ line vectors of measurement differences per applied measurement difference distribution, first and second parameter. Until now and during the preparation of iSHM footprints of [1], [2], piecewise monotonic data approximations are applied to the measured coupling scheme transfer function of eq. (1) having as a result the approximated coupling scheme transfer function that is given by

$$\overline{\overline{H_{d1,d2,i}^{\mathrm{OVLV},C,D,P}}}(f_q) = P\{\overline{H_{d1,d2,i}^{\mathrm{OVLV},C,D}}(f_q)\},\ q=1,\ldots,Q,\ i=1,\ldots,I \tag{2}$$

where $[\cdot]^P$ denotes the applied piecewise monotonic data approximation, say L1PMA or L2WPMA in this paper, and $P\{\cdot\}$ synopsizes the procedure of the applied piecewise monotonic data approximation. Therefore, the application of piecewise monotonic data approximations is concentrated in the Phase A of the BPMN diagram of iSHM while the results of the remaining Phases, which are illustrated as $I$ L1PMA cyan squares or $I$ L2WPMA magenta triangles on iSHM footprints of [2], are based on the approximated coupling scheme transfer function data.

In this paper, an application aspect of piecewise monotonic data approximations is proposed that has to do with the location of the application of piecewise monotonic data approximations across the Phases of the BPMN diagram of iSHM [34]. Conversely to the traditional case where piecewise monotonic data approximations are applied to the output results of the Phase A (say, the results of DHM), the new aspect of application suggests that the piecewise monotonic data approximations should be applied to the results of Phase B of the BPMN diagram of iSHM during the preparation of the iSHM footprints. More specifically, Phase B of the BPMN diagram should receive as input the output of the Phase A that is the measured coupling scheme transfer function $\overline{H_{d1,d2,i}^{\mathrm{OVLV},C,D}}(f_q)$ given by eq. (1). Phase B consists of the coupling scheme channel attenuation difference module $\Delta$ that computes the measured channel attenuation difference $\overline{\Delta \mathrm{A}_i^{\mathrm{G},C}}(f_q)$ between the measured coupling scheme transfer function of the examined real indicative OV LV BPL topology, say, the real indicative OV LV BPL urban case A in this paper, and the theoretical coupling scheme transfer function of the OV LV BPL "LOS" case, namely

$$\overline{\Delta \mathrm{A}_i^{\mathrm{G},C}}(f_q) = -\left[\overline{H_{d1,d2,i}^{\mathrm{OVLV},C,D}}(f_q) - H_{\text{"LOS" case}}^{\mathrm{OVLV},C}(f_q)\right],\ q=1,\ldots,Q,\ i=1,\ldots,I \tag{3}$$

Note that the coupling scheme channel attenuation difference of eq. (3) always remains greater or equal to zero [34]. During the preparation of similar iSHM footprints of [1], [2]

with the new aspect, piecewise monotonic data approximations are applied to the measured channel attenuation difference of eq. (3) having as a result the approximated channel attenuation difference given by

$$\overline{\overline{\Delta A_i^{G,C}}}(f_q) = P\{\overline{\Delta A_i^{G,C}}(f_q)\},\ q=1,\ldots,Q,\ i = 1, \ldots, I \quad (4)$$

Therefore, the application of piecewise monotonic data approximations during the new aspect leaves the results of the Phase A untouched whereas it focuses on the Phase B of the BPMN diagram of iSHM. Similarly to the traditional aspect, the results of the remaining Phases, which are based on the approximated channel attenuation difference data, are going to be illustrated as *I* L1PMA cyan squares or *I* L2WPMA magenta triangles on similar iSHM footprints to the ones of [2].

## 3. New Quantitative Methodology for Assessing the Mitigation Efficiency of Piecewise Monotonic Data Approximations against Measurement Differences via iSHM Footprints

In accordance with the BPMN diagram of iSHM [18] and during the preparation of iSHM footprints, Phase C computes all the related iSHM Weibull CASD MLEs of the examined real indicative OV LV BPL topology, namely either for the theoretical coupling scheme channel attenuation difference (i.e, $\hat{a}_{\mathrm{MLE,theor}}^{\mathrm{Weibull}}$ and $\hat{\beta}_{\mathrm{MLE,theor}}^{\mathrm{Weibull}}$) or the measured coupling scheme channel attenuation difference per measurement difference line vector *i* of eq. (3) (i.e, $\hat{a}_{\mathrm{MLE,meas},i}^{\mathrm{Weibull}}$ and $\hat{\beta}_{\mathrm{MLE,meas},i}^{\mathrm{Weibull}}$) or the approximated coupling scheme channel attenuation difference per measurement difference line vector *i* via the traditional aspect for given number of monotonic sections (or sign changes) (i.e, $\hat{a}_{\mathrm{MLE,approx,trad},i}^{\mathrm{Weibull}}$ and $\hat{\beta}_{\mathrm{MLE,approx,trad},i}^{\mathrm{Weibull}}$) or the approximated coupling scheme channel attenuation difference per measurement difference line vector *i* via the new aspect of eq. (4) for given number of L1PMA monotonic sections (or L2WPMA sign changes) (i.e, $\hat{a}_{\mathrm{MLE,approx,new},i}^{\mathrm{Weibull}}$ and $\hat{\beta}_{\mathrm{MLE,approx,new},i}^{\mathrm{Weibull}}$). In accordance with [36]-[38], the iSHM class map of OV LV BPL topologies, which acts as the graphical basis for the demonstration of all the kinds of iSHM footprints, is plotted in Fig. 1 of [2] with respect to $\hat{a}_{\mathrm{MLE}}^{\mathrm{Weibull}}$, $\hat{\beta}_{\mathrm{MLE}}^{\mathrm{Weibull}}$ and the average capacity of each OV LV BPL topology subclass when the default operation settings of [1], [34] and the modified BPL frequency range settings of [2] are assumed. Through the prism of iSHM footprints, the effect of measurement differences and the countermeasures of piecewise monotonic data approximations against the measurement differences have been illustrated in Figs. 2-7 of [2]. The qualitative assessment of piecewise monotonic data approximations via iSHM footprints has revealed their strong potential against measurement differences while the selection of the critical parameters of the numbers of L1PMA monotonic sections or L2WPMA sign changes can be made by visually assessing the proximity of the *I* Weibull CASD MLEs of their approximated coupling scheme transfer function data with respect to the theoretical Weibull CASD MLEs for given real indicative OV LV BPL topology.

In this paper, a quantitative methodology is proposed that benchmarks the measurement difference mitigation efficiency of piecewise monotonic data approximations in terms of the average percent distance of the *I* Weibull CASD MLEs of the approximated coupling scheme transfer function data with respect to the theoretical Weibull CASD MLEs for given real indicative OV LV BPL topology. To apply the new

quantitative methodology with respect to iSHM footprints and to finally select the critical intrinsic parameters of the piecewise monotonic data approximations (*i.e.*, the number of L1PMA monotonic sections and L2WPMA sign changes) that perform the best measurement difference mitigation, the following steps should be followed, namely:

1. *APDmd*: Given the real indicative OV LV BPL topology and $I$ measurement difference line vectors of the same intensity (*i.e.*, of the same maximum value $a_{\mathrm{CUD}}$ in this paper), the average percent distance of the measurement differences from the theoretical Weibull CASD MLEs is given by:

$$APDmd = 100\% \cdot \frac{\sum_{i=1}^{I} \sqrt{\left(\frac{\hat{a}_{\mathrm{MLE,meas},i}^{\mathrm{Weibull}} - \hat{a}_{\mathrm{MLE,theor}}^{\mathrm{Weibull}}}{\hat{a}_{\mathrm{MLE,theor}}^{\mathrm{Weibull}}}\right)^2 + \left(\frac{\hat{\beta}_{\mathrm{MLE,meas},i}^{\mathrm{Weibull}} - \hat{\beta}_{\mathrm{MLE,theor}}^{\mathrm{Weibull}}}{\hat{\beta}_{\mathrm{MLE,theor}}^{\mathrm{Weibull}}}\right)^2}}{I} \quad (5)$$

   This step is necessary because it evaluates the initial condition and defines the goal of all the iSHM footprints of the applied piecewise monotonic data approximations. Any countermeasures implemented should present average percent distances lower than the average percent distance of the measurement differences of eq. (5) so that these countermeasures are considered effective.

2. *APDta*: Given the real indicative OV LV BPL topology, $I$ measurement difference line vectors of the same intensity and the number of L1PMA monotonic sections (or L2WPMA sign changes), the average percent distance of the approximated data of the traditional aspect from the theoretical Weibull CASD MLEs is given by:

$$APDta = 100\% \cdot \frac{\sum_{i=1}^{I} \sqrt{\left(\frac{\hat{a}_{\mathrm{MLE,approx,trad},i}^{\mathrm{Weibull}} - \hat{a}_{\mathrm{MLE,theor}}^{\mathrm{Weibull}}}{\hat{a}_{\mathrm{MLE,theor}}^{\mathrm{Weibull}}}\right)^2 + \left(\frac{\hat{\beta}_{\mathrm{MLE,approx,trad},i}^{\mathrm{Weibull}} - \hat{\beta}_{\mathrm{MLE,theor}}^{\mathrm{Weibull}}}{\hat{\beta}_{\mathrm{MLE,theor}}^{\mathrm{Weibull}}}\right)^2}}{I} \quad (6)$$

3. *APDna*: Similarly to *APDta*, given the real indicative OV LV BPL topology, $I$ measurement difference line vectors of the same intensity and the number of L1PMA monotonic sections (or L2WPMA sign changes), the average percent distance between the approximated data of the new aspect and the theoretical Weibull CASD MLEs is given by:

$$APDna = 100\% \cdot \frac{\sum_{i=1}^{I} \sqrt{\left(\frac{\hat{a}_{\mathrm{MLE,approx,new},i}^{\mathrm{Weibull}} - \hat{a}_{\mathrm{MLE,theor}}^{\mathrm{Weibull}}}{\hat{a}_{\mathrm{MLE,theor}}^{\mathrm{Weibull}}}\right)^2 + \left(\frac{\hat{\beta}_{\mathrm{MLE,approx,new},i}^{\mathrm{Weibull}} - \hat{\beta}_{\mathrm{MLE,theor}}^{\mathrm{Weibull}}}{\hat{\beta}_{\mathrm{MLE,theor}}^{\mathrm{Weibull}}}\right)^2}}{I} \quad (7)$$

With reference to eqs. (5)-(7), it is obvious that interesting quantitative findings are going to be deduced in Sec. 4 where average percent distance comparisons can reveal: (i) the contamination degree due to the increasing measurement differences; (ii) the mitigation efficiency of the traditional aspect of the application of piecewise monotonic data approximations; (iii) the mitigation efficiency of the new aspect of the application of piecewise monotonic data approximations; and (iv) a benchmark comparison between the traditional aspect and the new one.

## 4. Numerical Results and Discussion

In this Section, numerical results that quantitatively assess the mitigation efficiency of piecewise monotonic data approximations against measurement differences on iSHM footprints of OV LV BPL topologies are first presented. On the basis of the

proposed quantitative assessment, the new methodology of the average percent distance is going to be tested while this new methodology will assess L1PMA and L2WPMA for both aspects of application (*i.e.*, either the traditional aspect or the new one). Similarly to [2], the countermeasures effect of L1PMA and L2WPMA of the traditional and new aspects is quantitatively benchmarked for given intensity of the measurement difference CUD while the impact of the number of L1PMA monotonic sections and the L2WPMA sign changes is here quantitatively assessed with respect to the mitigation of measurement differences. Similarly to [2], only the real indicative OV LV BPL urban case A is examined and 100 measurement difference line vector (*i.e.*, $I$=100) are applied.

### 4.1 iSHM Footprints due to Measurement Differences and the Countermeasures of Piecewise Monotonic Data Approximations (Traditional Aspect vs New Aspect)

As already been mentioned, the iSHM class map of OV LV BPL topologies, which is depicted in [36]-[38], acts as the graphical basis for the demonstration of the various iSHM footprints and is shown in Fig. 1. Similarly to [2], the iSHM footprint due to measurement differences of the arbitrary 5dB maximum value $a_{\mathrm{CUD}}$ for the real indicative OV LV BPL urban case A is also depicted in Fig. 1 as superimposed white circles on the iSHM class map as well as the iSHM footprint due to the application of L1PMA of the traditional aspect against the aforementioned measurement differences is shown as superimposed cyan squares when 4 monotonic sections are assumed. In Fig. 2, similar figure with Fig. 1 is plotted but for the case of L2WPMA of the traditional aspect when 4 sign changes are applied and superimposed magenta triangles are shown instead of cyan squares. Note that Figs. 1 and 2 are the same with Figs. 2 and 3 of [2] for: (i) comparison reasons between the traditional and the new aspect; and (ii) the demonstration of the proposed quantitative analysis. In Figs. 3 and 4, same plots with the respective Figs. 1 and 2 but for the new aspect. Here, it should be reminded that an iSHM footprint due to zero measurement differences consists of $I$ white circles that all circles coincide at the theoretical values $\hat{a}_{\mathrm{MLE,theor}}^{\mathrm{Weibull}}$ and $\hat{\beta}_{\mathrm{MLE,theor}}^{\mathrm{Weibull}}$ of the real indicative OV LV BPL urban case A that is the optimum case and the iSHM footprint goal of the application of piecewise monotonic data approximations.

By comparing iSHM footprints of Figs 1-4, each iSHM footprint due to measurement differences consists of 100 white circles forming a segmented white region that starts from the theoretical values $\hat{a}_{\mathrm{MLE,theor}}^{\mathrm{Weibull}}$ and $\hat{\beta}_{\mathrm{MLE,theor}}^{\mathrm{Weibull}}$ of the real indicative OV LV BPL urban case A where each white circle corresponds to one measurement difference line vector. Regardless of the applied aspect, each cyan square and each magenta triangle is the graphical approximation result on the iSHM footprint for each white circle when L1PMA and L2WPMA are applied, respectively.

In accordance with [2], the qualitative approximation success of L1PMA and L2WPMA has been evaluated by the upper right shift of the respective iSHM footprints towards the theoretical values $\hat{a}_{\mathrm{MLE,theor}}^{\mathrm{Weibull}}$ and $\hat{\beta}_{\mathrm{MLE,theor}}^{\mathrm{Weibull}}$ of the real indicative OV LV BPL urban case A. Although the mitigation of measurement differences is clear after the application of the piecewise monotonic data approximations of both aspects, the qualitative assessment is not enough to recognize which of the iSHM footprints achieves the best mitigation. The quantitative methodology of Sec.3 can offer the required metrics to carefully benchmark the iSHM footprints after the application of piecewise monotonic data approximations and aspects of Figs. 1-4. The benchmark results of L1PMA and L2WPMA when traditional and new aspects are applied are

reported in Table 1 after the application of the quantitative methodology of Sec. 3 to Figs. 1-4.

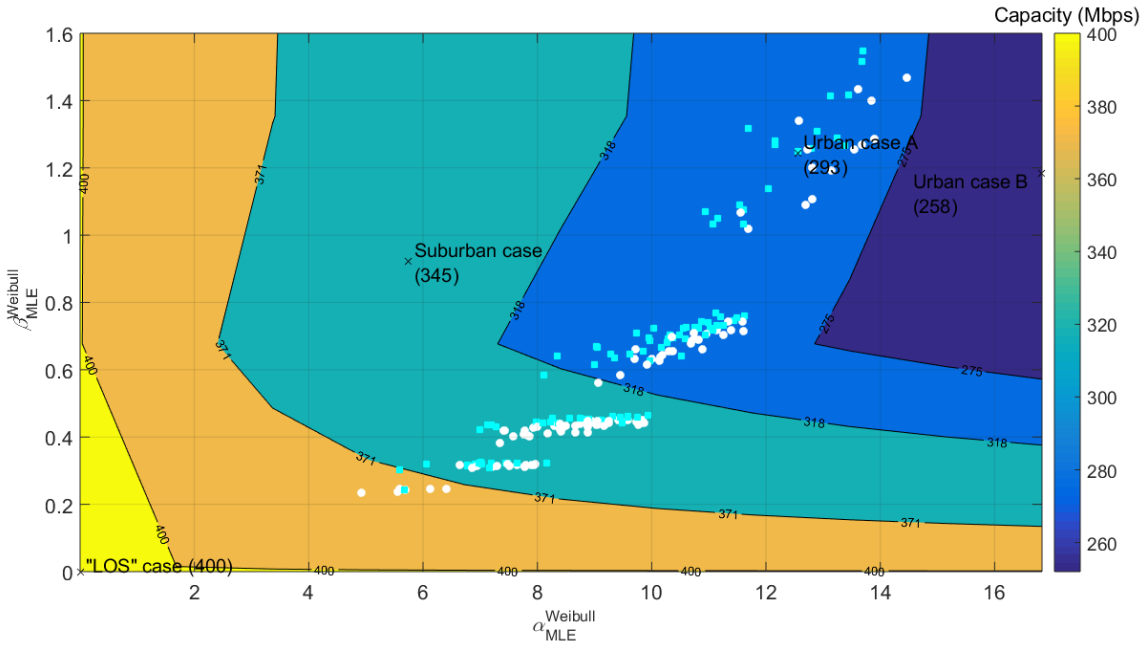


**Fig. 1**. iSHM footprints of the real indicative OV LV BPL urban case A when 3-30MHz frequency band, 1MHz frequency subchannel spacing, WtG[1] coupling scheme, FCC Part 15, CUD measurement differences of maximum value $a_{CUD}$ = 5dB (white circles) are assumed and L1PMA of the traditional aspect of 4 monotonic sections (cyan squares) is applied [2].

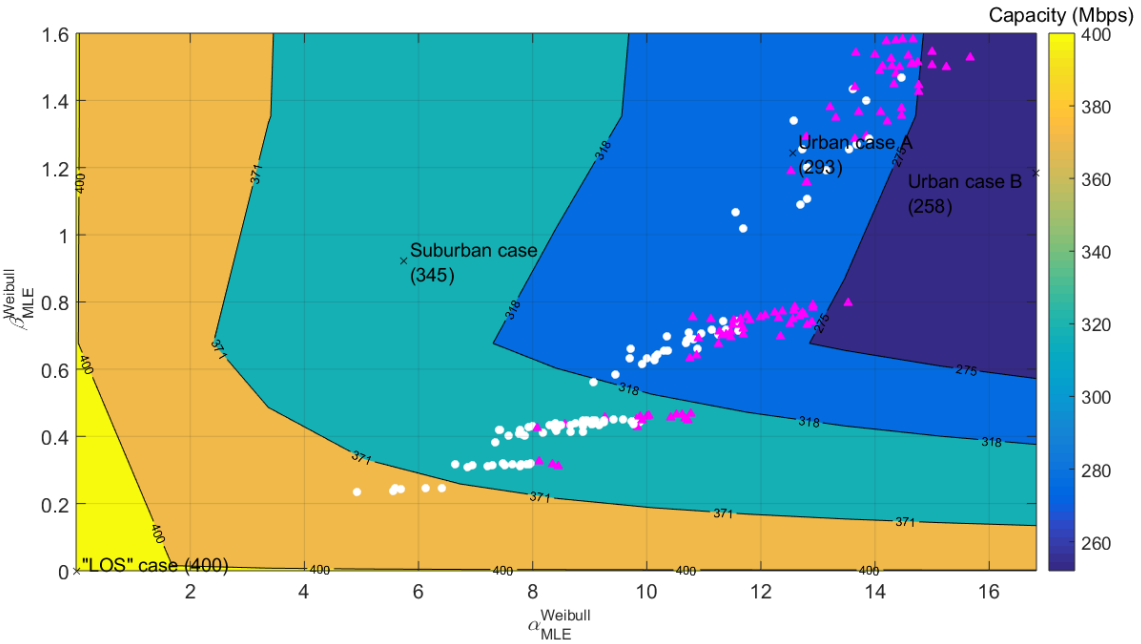


**Fig. 2**. Same plot with Fig. 1 but for L2WPMA of the traditional aspect of 4 sign changes (magenta triangles) [2].

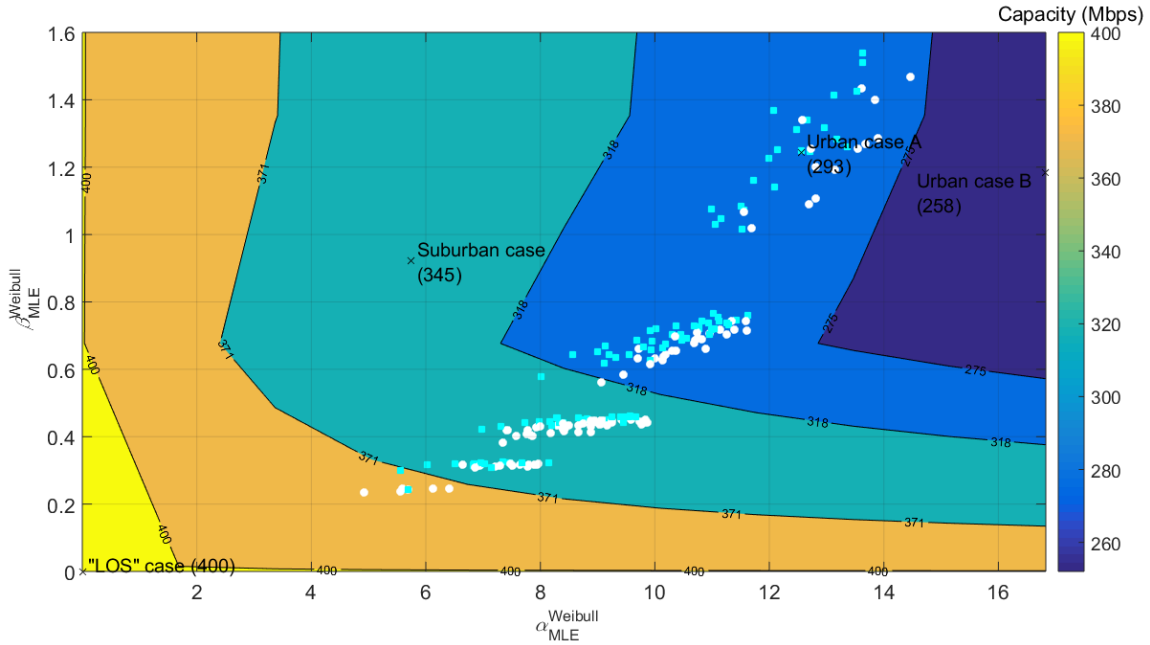


**Fig. 3**. Same plot with Fig. 1 but for L1PMA of the new aspect of 4 monotonic sections (cyan squares).

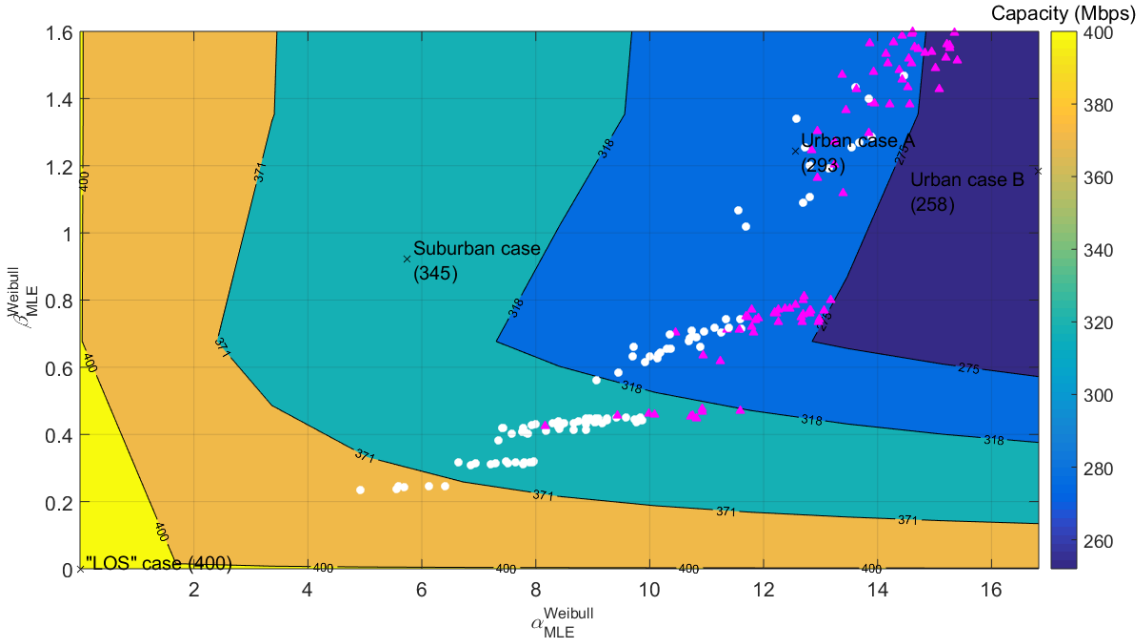


**Fig. 4**. Same plot with Fig. 2 but for L2WPMA of the new aspect of 4 sign changes (magenta triangles).

Table 1
Quantitative methodology benchmark results for L1PMA and L2WPMA when Traditional and New Aspects are Applied

| **Number of L1PMA Monotonic Sections / L2WPMA Sign Changes** | **Measurement Differences (maximum value $a_{CUD}$=5dB)** | **Traditional Aspect** | | **New Aspect** | |
|---|---|---|---|---|---|
| | | **L1PMA** | **L2WPMA** | **L1PMA** | **L2WPMA** |
| | ***APDmd*** **(%)** | ***APDta*** **(%)** | ***APDta*** **(%)** | ***APDna*** **(%)** | ***APDna*** **(%)** |
| 4 | 61.22 | 53.90 | 38.67 | 51.98 | 36.09 |

By comparing the benchmark results of Table 1 with Figs. 1-4, it is evident that L1PMA and L2WPMA achieve to mitigate the measurement differences regardless of the aspect applied. Both piecewise monotonic data approximations of this paper shift their iSHM footprints up right in comparison with the iSHM footprint due to measurement differences. Note that the approximated iSHM footprints now lie closer to the theoretical values $\hat{a}_{\mathrm{MLE,theor}}^{\mathrm{Weibull}}$ and $\hat{\beta}_{\mathrm{MLE,theor}}^{\mathrm{Weibull}}$ of the real indicative OV LV BPL urban case A in comparison with the iSHM footprints due to measurement differences. Numerically, *APDmd* of the assumed measurement differences is equal to 61.22% whilst the worst performance of piecewise monotonic data approximations is achieved by L1PMA of the traditional aspect with *APDta* that is equal to 53.90%.

As the traditional and new aspects are here benchmarked, it is clear that the piecewise monotonic data approximations of the new aspect better mitigate the measurement differences in comparison with the respective ones of the traditional aspect. Numerically, L1PMA of the traditional aspect presents higher *APDta*, which is equal to 53.90%, in comparison with the *APDna* of L1PMA of the new aspect that is equal to 51.98%. Similarly, L2WPMA of the traditional aspect presents higher *APDta*, which is equal to 38.67%, in comparison with the *APDna* of L2WPMA of the new aspect that is equal to 36.09%. Anyway, the previous numerical results can also be observed in the previous Figs. 1-4. Piecewise monotonic data approximations of the new aspect handle more unbiased data in comparison with ones of the traditional aspect since the coupling scheme transfer function of the OV LV BPL "LOS" case acts as a background noise for the coupling scheme transfer function of the other OV LV BPL topologies. When 4 monotonic sections or sign changes are assumed, the best mitigation performance against measurement differences is achieved by L2WPMA of the new aspect.

From the previous analysis, it is evident that during the quantitative methodology there is no need for visually comparing the iSHM footprints due to the measurement differences and the iSHM footprints after the application of piecewise monotonic data approximations since APD metrics can securely allow the selection of the most suitable piecewise monotonic data approximation as well as its critical parameters for both aspects (*i.e.*, L1PMA monotonic sections or L2WPMA sign changes). Since the qualitative analysis has been fulfilled in [2], only tables of APD metrics are presented hereafter in order to assess the performance of the various versions of the piecewise monotonic data approximations. In the following subsection, the selection of the

aforementioned critical parameters of piecewise monotonic data approximations is justified by the APD metrics and visually verified by Figs. 4(a)-(i) and 5(a)-(i) of [2].

### 4.2 The Quantitative Methodology for Defining the Number of L1PMA Monotonic Sections and L2WPMA Sign Changes

Already been identified in [2], [10], [26], [39], [40], the selection of the numbers of L1PMA monotonic sections and of L2WPMA sign changes has a significant impact on the mitigation performance of measurement differences. Also, this selection of the critical parameters of the piecewise monotonic data approximations can remain untouchable despite the different intensities of measurement differences applied with satisfactory performance unless adaptive techniques such those presented in [10], [11], [26], [39], [40] should be applied.

With reference to Figs. 4(a)-(i) and 5(a)-(i) of [2] as well as the proposed quantitative methodology of Sec. 3, APD metrics of: (i) the applied measurement differences of the arbitrary 6dB maximum value $a_{\mathrm{CUD}}$ for the real indicative OV LV BPL urban case A; and (ii) the piecewise monotonic data approximations of both the aspects; are here reported in Table 2 when the numbers of L1PMA monotonic sections and L2WPMA sign changes range from 1 to 9.

From Table 2, several interesting remarks that agree with the visual findings of Figs. 4(a)-(i) and 5(a)-(i) of [2], can be pointed out, namely:

- Depending on the number of L1PMA monotonic sections and L2WPMA sign changes, different mitigation performances can be observed among the available piecewise monotonic data approximations. The aforementioned result that is proven by the APD metrics of Table 2 has also been verified by the visual analysis of Figs. 4(a)-(i) and 5(a)-(i) of [2].
- As the application of L1PMA of the traditional aspect is concerned, its best mitigation performance with *APDta* of 38.48% is observed when one monotonic section is adopted. This *APDta* result is the best one among all the cases examined. Anyway, the same number of L1PMA monotonic sections has been verified for its mitigation performance by the visual examination of Figs. 4(a)-(i). As the number of monotonic sections increases so does *APDta* thus indicating that the relatively high intensity of measurement differences that is adopted in this subsection (*i.e.*, maximum value $a_{\mathrm{CUD}}$ of 6dB) requires the rough approximation provided by the assumption of 1 monotonic section. The overapproximation, which is defined in [2], occurs when the number of L1PMA monotonic sections of the traditional aspect is greater than 5 (*i.e.*, black background cells of the third and fourth columns of Table 2).
- As the application of L2WPMA of the traditional aspect is regarded, its best mitigation performance with *APDta* of 39.54% is observed when four or five sign changes are adopted. With reference to Fig. 5(e) of [2], the same number of L2WPMA sign changes has been validated for its mitigation performance by the visual examination. As the number of sign changes increases *APDta* first presents significant high values that are even higher than the respective *APDmds* (*i.e.*, black background cells of the fifth and sixth columns of Table 2), second starts to decrease till 39.54% of four or five sign changes and then increases tending to

Table 2
Quantitative methodology benchmark results for L1PMA and L2WPMA when Traditional and New Aspects are Applied for various Numbers of L1PMA Monotonic Sections and L2WPMA Sign Changes

| **Number of L1PMA Monotonic Sections / L2WPMA Sign Changes** | **Measurement Differences (maximum value $a_{CUD}$=6dB)** | **Traditional Aspect** | | | | **New Aspect** | |
|---|---|---|---|---|---|---|---|
| | | **L1PMA** | | **L2WPMA** | | **L1PMA** | **L2WPMA** |
| | ***APDmd* (%)** | ***APDta* (%)** | **Reference Figure of [2]** | ***APDta* (%)** | **Reference Figure of [2]** | ***APDna* (%)** | ***APDna* (%)** |
| 1 | 68.63 | 38.48 | Fig. 4(a) | 111.58 | Fig. 5(a) | 40.19 | 118.94 |
| 2 | | 45.98 | Fig. 4(b) | 99.64 | Fig. 5(b) | 44.01 | 106.67 |
| 3 | | 57.67 | Fig. 4(c) | 51.58 | Fig. 5(c) | 55.63 | 45.94 |
| 4 | | 58.17 | Fig. 4(d) | 39.54 | Fig. 5(d) | 55.95 | 39.37 |
| 5 | | 62.04 | Fig. 4(e) | 39.54 | Fig. 5(e) | 59.57 | 39.37 |
| 6 | | 69.46 | Fig. 4(f) | 46.25 | Fig. 5(f) | 68.06 | 39.69 |
| 7 | | 69.51 | Fig. 4(g) | 46.25 | Fig. 5(g) | 68.11 | 39.69 |
| 8 | | 71.46 | Fig. 4(h) | 55.15 | Fig. 5(h) | 70.94 | 46.72 |
| 9 | | 71.46 | Fig. 4(i) | 55.15 | Fig. 5(i) | 70.94 | 46.72 |

a state of overapproximation. In contrast with L1PMA of the traditional aspect, L2WPMA tends to approximate the spectral notches of the coupling scheme transfer function data by avoiding the rough approximation of 1 monotonic section of L1PMA.

- As the application of L1PMA of the new aspect is concerned, its *APDna* behavior presents similarities with *APDta* of the L1PMA of the traditional aspect with respect to the number of monotonic sections. Indeed, the best *APDna* of the L1PMA of the new aspect is equal to 40.19% when one monotonic section is adopted. In all the numbers of monotonic sections examined, L1PMA of the new aspect presents better *APDna* than *APDta* of the L1PMA of the traditional aspect except the case of the one monotonic section. Anyway, L1PMA of the new aspect achieves to mitigate measurement differences of the maximum value $a_{CUD}$ of 6dB even if 7 monotonic sections are assumed. Above 7 monotonic sections, its *APDna* exceeds *APDmd* (*i.e.*, black background cells of the seventh column of Table 2).
- As the application of L2WPMA of the new aspect is regarded, its best mitigation performance with *APDna* of 39.37% is observed when four or five sign changes are adopted that is the same number of sign changes of L2WPMA of the traditional aspect. Below 3 monotonic sections, its *APDna* exceeds *APDmd* (*i.e.*, black background cells of the eighth column of Table 2). For the monotonic sections that *APDna* is lower than *APDmd*, *APDna* of L2WPMA of the new

aspect always presents better values in comparison with *APDta* of L2WPMA of the traditional aspect.

Note that the numbers of 1 L1PMA monotonic section for both aspects and 5 L2WPMA sign changes for both aspects are going to be adopted in the following analysis. In accordance with [2], the aforementioned numbers can be treated as the basis for the respective piecewise monotonic data approximations regardless of the intensity of the measurement differences. In order to check the mitigation efficiency of L1PMA and L2WPMA of both aspects against different intensities of measurement differences, their performance is assessed through the quantitative methodology on the basis of respective iSHM footprints.

### 4.3 The Quantitative Methodology for L1PMA and L2WPMA iSHM Footprints of both Aspects when Different Intensities of Measurement Differences Occur

In accordance with Figs. 6 and 7 of [2], the mitigation performance of L1PMA and L2WPMA of the traditional aspect against the measurement differences has been visually proven to be important when measurement differences remain very high. Anyway, the promising results regarding the mitigation of higher measurement differences by L1PMA and L2WPMA of the traditional aspect was expected after the determination of respective monotonic sections and sign changes in Sec.3.3 of [2] for maximum value $a_{\mathrm{CUD}}$ of 6dB that is anyway sufficiently high. The aforementioned qualitative observations of [2] require the quantitative validation of this Section.

Unlike [2], in Table 3, APD metrics of: (i) the applied measurement differences of maximum values $a_{\mathrm{CUD}}$ that range from 0dB to 15dB for the real indicative OV LV BPL urban case A; and (ii) the results of the application of piecewise monotonic data approximations of both aspects; are here reported when the numbers of L1PMA monotonic sections and L2WPMA sign changes are equal to 1 and 5, respectively.

From Table 3, it is clear that the increasing maximum value $a_{\mathrm{CUD}}$ of CUD measurement differences entail significant increase of *APDmd*. Since L1PMA monotonic sections and L2WPMA sign changes have been defined when the relatively high measurement differences of Sec. 4.2 have been assumed, L1PMA and L2WPMA fail to mitigate the low measurement differences of maximum value $a_{\mathrm{CUD}}$ of 1dB and 2dB. Here, the philosophy of the adaptive monotonic sections and sign changes, which have been proposed in [10], [11], can also be applied in iSHM footprints so that even the low measurement differences of maximum value $a_{\mathrm{CUD}}$ of 1dB and 2dB can be mitigated by piecewise monotonic data approximations.

In contrast with the situation occurs during the study of the very low measurement differences, L1PMA and L2WPMA can safely mitigate measurement differences whose maximum value $a_{\mathrm{CUD}}$ remains higher than 2dB regardless of the aspect adopted. In fact, for the high measurement differences, L1PMA of the traditional aspect when one monotonic section is applied achieves the best *APDta* in comparison with the APD metrics of the other examined piecewise monotonic data approximations till approximately maximum values $a_{\mathrm{CUD}}$ of 10dB (cyan background cells of Table 3). For the very high measurement differences, L1PMA of the new aspect when one monotonic section is again applied starts to present the best *APDna* in comparison with the ones of the other examined piecewise monotonic data approximations. Anyway, the mitigation performance of all the examined piecewise monotonic data approximations mitigate measurement differences when maximum values $a_{\mathrm{CUD}}$ are greater than 2dB.

Table 3
Quantitative methodology benchmark results for L1PMA and L2WPMA when Traditional and New Aspects are Applied
(maximum value $a_{\mathrm{CUD}}$ ranges from 0dB to 15dB, numbers of L1PMA monotonic sections and L2WPMA sign changes are equal to 1 and 5, respectively)

| **Maximum Value $a_{\mathrm{CUD}}$ of Measurement Differences (dB)** | **Measurement Differences** | **Traditional Aspect** | | **New Aspect** | |
|---|---|---|---|---|---|
| | | **L1PMA** | **L2WPMA** | **L1PMA** | **L2WPMA** |
| | ***APDmd* (%)** | ***APDta* (%)** | ***APDta* (%)** | ***APDna* (%)** | ***APDna* (%)** |
| 0 | 0 | 19.35 | 15.92 | 18.74 | 17.12 |
| 1 | 7.99 | 18.95 | 18.58 | 19.12 | 18.80 |
| 2 | 16.57 | 19.67 | 23.18 | 20.24 | 22.35 |
| 3 | 32.23 | 20.43 | 24.41 | 21.73 | 24.42 |
| 4 | 46.39 | 24.94 | 32.55 | 25.59 | 31.11 |
| 5 | 61.22 | 33.78 | 38.67 | 34.57 | 36.09 |
| 6 | 68.63 | 38.48 | 39.54 | 40.19 | 39.37 |
| 7 | 72.73 | 39.05 | 41.40 | 39.16 | 42.64 |
| 8 | 85.35 | 41.42 | 46.67 | 41.61 | 45.56 |
| 9 | 84.34 | 43.93 | 48.43 | 44.34 | 49.25 |
| 10 | 90.42 | 48.98 | 50.90 | 49.10 | 50.10 |
| 11 | 96.07 | 46.94 | 51.24 | 46.47 | 55.05 |
| 12 | 99.99 | 52.04 | 55.25 | 52.32 | 56.82 |
| 13 | 101.48 | 50.14 | 57.20 | 49.57 | 59.39 |
| 14 | 105.69 | 59.39 | 63.10 | 59.20 | 64.35 |
| 15 | 110.69 | 58.65 | 59.95 | 58.58 | 63.99 |

As L2WPMA is examined, mixed performance results occur between the traditional and new aspect. In general terms about L2WPMA, the traditional aspect is preferred when high measurement differences occur whereas the new aspect is used in the other cases.

Through the prism of the new quantitative methodology, it is evident that piecewise monotonic data approximations can easily mitigate measurement differences when piecewise monotonic data approximations are well calibrated in terms of their critical intrinsic parameters. Depending on the applied piecewise monotonic data approximations and the intensity of measurement differences as previously analyzed, the selection among the available piecewise monotonic data approximations and aspects changes.

## 5. Conclusions

After the proposal of the quantitative methodology of this companion paper, the reliability of BPL data that feed the business analytics and the tools of the SG is further enhanced. Towards the enhancement of the data quality and the data cleaning from the application of piecewise monotonic data approximations, such as L1PMA and

L2WPMA, the new aspect of applying piecewise monotonic data approximations can successfully mitigate measurement differences under conditions. With reference to iSHM footprints, it has been revealed that L1PMA and L2WPMA always mitigate measurements differences above a low threshold of 2dB while their performance becomes significant when measurement differences are important since the generated data of high measurement difference contamination are considered useless without a restoration. Finally, the interoperability of the qualitative and quantitative assessments of piecewise monotonic data approximations via iSHM footprints can be considered invaluable in order to ensure the data quality of the business analytics while the new aspects are added to the quiver of the available mitigation techniques against the measurement differences.

## CONFLICTS OF INTEREST

The author declares that there is no conflict of interests regarding the publication of this paper.

## References

[1] A. G. Lazaropoulos, "Business Analytics and IT in Smart Grid – Part 1: The Impact of Measurement Differences on the iSHM Class Map Footprints of Overhead Low-Voltage Broadband over Power Lines Topologies," *Trends in Renewable Energy*, vol. 6, no. 2, pp. 146-176, May 2020.

[2] A. G. Lazaropoulos, "Business Analytics and IT in Smart Grid – Part 2: The Qualitative Mitigation Impact of Piecewise Monotonic Data Approximations on the iSHM Class Map Footprints of Overhead Low-Voltage Broadband over Power Lines Topologies Contaminated by Measurement Differences," *Trends in Renewable Energy*, vol. 6, no. 2, pp. 177-203, May 2020.

[3] A. G. Lazaropoulos, "Factors Influencing Broadband Transmission Characteristics of Underground Low-Voltage Distribution Networks," *IET Commun.*, vol. 6, no. 17, pp. 2886-2893, Nov. 2012.

[4] A. G. Lazaropoulos, "Deployment Concepts for Overhead High Voltage Broadband over Power Lines Connections with Two-Hop Repeater System: Capacity Countermeasures against Aggravated Topologies and High Noise Environments," *Progress in Electromagnetics Research B*, vol. 44, pp. 283-307, 2012. [Online]. Available: http://www.jpier.org/PIERB/pierb44/13.12081104.pdf

[5] A. G. Lazaropoulos, "Broadband Performance Metrics and Regression Approximations of the New Coupling Schemes for Distribution Broadband over Power Lines (BPL) Networks," *Trends in Renewable Energy*, vol. 4, no. 1, pp. 43-73, Jan. 2018. [Online]. Available: http://futureenergysp.com/index.php/tre/article/view/59/pdf

[6] A. G. Lazaropoulos, "Wireless Sensor Network Design for Transmission Line Monitoring, Metering and Controlling Introducing Broadband over PowerLines-enhanced Network Model (BPLeNM)," *ISRN Power Engineering*, vol. 2014, Article ID 894628, 22 pages, 2014. doi:10.1155/2014/894628. [Online].

Available: http://www.hindawi.com/journals/isrn.power.engineering/2014/894628/

[7] A. G. Lazaropoulos, "Improvement of Power Systems Stability by Applying Topology Identification Methodology (TIM) and Fault and Instability Identification Methodology (FIIM)–Study of the Overhead Medium-Voltage Broadband over Power Lines (OV MV BPL) Networks Case," *Trends in Renewable Energy*, vol. 3, no. 2, pp. 102-128, Apr. 2017. [Online]. Available: http://futureenergysp.com/index.php/tre/article/view/34

[8] A. G. Lazaropoulos, "Smart Energy and Spectral Efficiency (SE) of Distribution Broadband over Power Lines (BPL) Networks – Part 1: The Impact of Measurement Differences on SE Metrics," *Trends in Renewable Energy*, vol. 4, no. 2, pp. 125-184, Aug. 2018. [Online]. Available: http://futureenergysp.com/index.php/tre/article/view/76/pdf

[9] A. G. Lazaropoulos, "Detection of Energy Theft in Overhead Low-Voltage Power Grids – The Hook Style Energy Theft in the Smart Grid Era," *Trends in Renewable Energy*, vol. 5, no. 1, pp. 12-46, Oct. 2018. [Online]. Available: http://futureenergysp.com/index.php/tre/article/view/81/pdf

[10] A. G. Lazaropoulos, "Power Systems Stability through Piecewise Monotonic Data Approximations – Part 1: Comparative Benchmarking of L1PMA, L2WPMA and L2CXCV in Overhead Medium-Voltage Broadband over Power Lines Networks," *Trends in Renewable Energy*, vol. 3, no. 1, pp. 2-32, Jan. 2017. [Online]. Available: http://futureenergysp.com/index.php/tre/article/view/29/34

[11] A. G. Lazaropoulos, "Power Systems Stability through Piecewise Monotonic Data Approximations – Part 2: Adaptive Number of Monotonic Sections and Performance of L1PMA, L2WPMA and L2CXCV in Overhead Medium-Voltage Broadband over Power Lines Networks," *Trends in Renewable Energy*, vol. 3, no. 1, pp. 33-60, Jan. 2017. [Online]. Available: http://futureenergysp.com/index.php/tre/article/view/30/35

[12] A. G. Lazaropoulos and P. G. Cottis, "Transmission characteristics of overhead medium voltage power line communication channels," *IEEE Trans. Power Del.*, vol. 24, no. 3, pp. 1164-1173, Jul. 2009.

[13] A. G. Lazaropoulos and P. G. Cottis, "Capacity of overhead medium voltage power line communication channels," *IEEE Trans. Power Del.*, vol. 25, no. 2, pp. 723-733, Apr. 2010.

[14] A. G. Lazaropoulos and P. G. Cottis, "Broadband transmission via underground medium-voltage power lines-Part I: transmission characteristics," *IEEE Trans. Power Del.*, vol. 25, no. 4, pp. 2414-2424, Oct. 2010.

[15] A. G. Lazaropoulos and P. G. Cottis, "Broadband transmission via underground medium-voltage power lines-Part II: capacity," *IEEE Trans. Power Del.*, vol. 25, no. 4, pp. 2425-2434, Oct. 2010.

[16] A. G. Lazaropoulos, "Broadband transmission and statistical performance properties of overhead high-voltage transmission networks," *Hindawi Journal of Computer Networks and Commun.*, 2012, article ID 875632, 2012. [Online]. Available: http://www.hindawi.com/journals/jcnc/aip/875632/

[17] A. G. Lazaropoulos, "Towards Modal Integration of Overhead and Underground Low-Voltage and Medium-Voltage Power Line Communication Channels in the Smart Grid Landscape: Model Expansion, Broadband Signal Transmission Characteristics, and Statistical Performance Metrics (Invited Paper)," *ISRN Signal*

*Processing*, vol. 2012, Article ID 121628, pp. 1-17, 2012. [Online]. Available: http://www.hindawi.com/isrn/sp/2012/121628/

[18] A. G. Lazaropoulos, "Statistical Broadband over Power Lines Channel Modeling – Part 1: The Theory of the Statistical Hybrid Model," *Progress in Electromagnetics Research C*, vol. 92, pp. 1-16, 2019. [Online]. Available: http://www.jpier.org/PIERC/pierc92/01.19012902.pdf

[19] A. G. Lazaropoulos, "Statistical Broadband over Power Lines (BPL) Channel Modeling – Part 2: The Numerical Results of the Statistical Hybrid Model," *Progress in Electromagnetics Research C*, vol. 92, pp. 17-30, 2019. [Online]. Available: http://www.jpier.org/PIERC/pierc92/02.19012903.pdf

[20] A. G. Lazaropoulos, "Enhancing the Statistical Hybrid Model Performance in Overhead and Underground Medium Voltage Broadband over Power Lines Channels by Adopting Empirical Channel Attenuation Statistical Distribution," *Trends in Renewable Energy*, vol. 5, no. 2, pp. 181-217, 2019. [Online]. Available: http://futureenergysp.com/index.php/tre/article/view/96/pdf

[21] A. G. Lazaropoulos, "Main Line Fault Localization Methodology in Smart Grid–Part 1: Extended TM2 Method for the Overhead Medium-Voltage Broadband over Power Lines Networks Case," *Trends in Renewable Energy*, vol. 3, no. 3, pp. 2-25, Dec. 2017. [Online]. Available: http://futureenergysp.com/index.php/tre/article/view/36

[22] A. G. Lazaropoulos, "Main Line Fault Localization Methodology in Smart Grid–Part 2: Extended TM2 Method, Measurement Differences and L1 Piecewise Monotonic Data Approximation for the Overhead Medium-Voltage Broadband over Power Lines Networks Case," *Trends in Renewable Energy*, vol. 3, no. 3, pp. 26-61, Dec. 2017. [Online]. Available: http://futureenergysp.com/index.php/tre/article/view/37

[23] A. G. Lazaropoulos, "Main Line Fault Localization Methodology in Smart Grid–Part 3: Main Line Fault Localization Methodology (MLFLM)," *Trends in Renewable Energy*, vol. 3, no. 3, pp. 62-81, Dec. 2017. [Online]. Available: http://futureenergysp.com/index.php/tre/article/view/38

[24] A. G. Lazaropoulos, "Main Line Fault Localization Methodology (MLFLM) in Smart Grid–The Underground Medium- and Low-Voltage Broadband over Power Lines Networks Case," *Trends in Renewable Energy*, vol. 4, no. 1, pp. 15-42, Dec. 2017. [Online]. Available: http://futureenergysp.com/index.php/tre/article/view/45

[25] A. G. Lazaropoulos, "Smart Energy and Spectral Efficiency (SE) of Distribution Broadband over Power Lines (BPL) Networks – Part 2: L1PMA, L2WPMA and L2CXCV for SE against Measurement Differences in Overhead Medium-Voltage BPL Networks," *Trends in Renewable Energy*, vol. 4, no. 2, pp. 185-212, Aug. 2018. [Online]. Available: http://futureenergysp.com/index.php/tre/article/view/77/pdf

[26] A. G. Lazaropoulos, "Measurement Differences, Faults and Instabilities in Intelligent Energy Systems – Part 2: Fault and Instability Prediction in Overhead High-Voltage Broadband over Power Lines Networks by Applying Fault and Instability Identification Methodology (FIIM)," *Trends in Renewable Energy*, vol. 2, no. 3, pp. 113-142, Oct. 2016. [Online]. Available: http://futureenergysp.com/index.php/tre/article/view/27/33

[27] A. G. Lazaropoulos, "Special Cases during the Detection of the Hook Style Energy Theft in Overhead Low-Voltage Power Grids through HS-DET Method – Part 1: High Measurement Differences, Very Long Hook Technique and "Smart" Hooks," *Trends in Renewable Energy*, vol. 5, no. 1, pp. 60-89, Jan. 2019. [Online]. Available: http://futureenergysp.com/index.php/tre/article/view/82/pdf

[28] A. G. Lazaropoulos, "Special Cases during the Detection of the Hook Style Energy Theft in Overhead Low-Voltage Power Grids through HS-DET Method – Part 2: Different Measurement Differences, Feint "Smart" Hooks and Hook Interconnection Issues," *Trends in Renewable Energy*, vol. 5, no. 1, pp. 90-116, Jan. 2019. [Online]. Available: http://futureenergysp.com/index.php/tre/article/view/83/pdf

[29] A. G. Lazaropoulos, "Underground Distribution BPL Connections with (N + 1)-hop Repeater Systems: A Novel Capacity Mitigation Technique," *Elsevier Computers and Electrical Engineering*, vol. 40, pp. 1813-1826, 2014.

[30] I. C. Demetriou, "An application of best *L*1 piecewise monotonic data approximation to signal restoration," *IAENG International Journal of Applied Mathematics*, vol. 53, no. 4, pp. 226-232, 2013.

[31] I. C. Demetriou, "L1PMA: A Fortran 77 Package for Best L1 Piecewise Monotonic Data Smoothing," *Computer Physics Communications*, vol. 151, no. 1, pp. 315-338, 2003.

[32] I. C. Demetriou, "A Decomposition Theorem for the Least Squares Piecewise Monotonic Data Approximation Problem," *Springer Approximation and Optimization*, pp. 119–134, 2019.

[33] I. C. Demetriou and M. J. D. Powell, "Least squares smoothing of univariate data to achieve piecewise monotonicity", *IMA Journal of Numerical Analysis*, vol. 11, no. 3, pp. 411-432, 1991.

[34] A. G. Lazaropoulos, "Statistical Channel Modeling of Overhead Low Voltage Broadband over Power Lines (OV LV BPL) Networks – Part 1: The Theory of Class Map Footprints of Real OV LV BPL Topologies, Branch Line Faults and Hook-Style Energy Thefts," *Trends in Renewable Energy*, vol. 6, no. 1, pp. 61-87, Mar. 2020. [Online]. Available: http://futureenergysp.com/index.php/tre/article/download/112/pdf

[35] A. G. Lazaropoulos, "New Coupling Schemes for Distribution Broadband over Power Lines (BPL) Networks," *Progress in Electromagnetics Research B*, vol. 71, pp. 39-54, 2016. [Online]. Available: http://www.jpier.org/PIERB/pierb71/02.16081503.pdf

[36] A. G. Lazaropoulos, "Virtual Indicative Broadband over Power Lines Topologies for Respective Subclasses by Adjusting Channel Attenuation Statistical Distribution Parameters of Statistical Hybrid Models – Part 2: Numerical Results for the Overhead and Underground Medium-Voltage Power Grids," *Trends in Renewable Energy*, vol. 5, no. 3, pp. 258-281, Aug. 2019. [Online]. Available: http://futureenergysp.com/index.php/tre/article/view/100/pdf

[37] A. G. Lazaropoulos, "Virtual Indicative Broadband over Power Lines Topologies for Respective Subclasses by Adjusting Channel Attenuation Statistical Distribution Parameters of Statistical Hybrid Models – Part 3: The Case of Overhead Transmission Power Grids," *Trends in Renewable Energy*, vol. 5, no. 3, pp. 282-306, Aug. 2019. [Online]. Available: http://futureenergysp.com/index.php/tre/article/view/101/pdf

[38] A. G. Lazaropoulos, "Statistical Channel Modeling of Overhead Low Voltage Broadband over Power Lines (OV LV BPL) Networks – Part 2: The Numerical Results of Class Map Footprints of Real OV LV BPL Topologies, Branch Line Faults and Hook Style Energy Thefts," *Trends in Renewable Energy*, vol. 6, no. 1, pp. 88-109, Mar. 2020. [Online]. Available: http://futureenergysp.com/index.php/tre/article/download/113/pdf

[39] A. G. Lazaropoulos, "Best L1 Piecewise Monotonic Data Approximation in Overhead and Underground Medium-Voltage and Low-Voltage Broadband over Power Lines Networks: Theoretical and Practical Transfer Function Determination," Hindawi Journal of Computational Engineering, vol. 2016, Article ID 6762390, 24 pages, 2016. doi:10.1155/2016/6762390. [Online]. Available: https://www.hindawi.com/journals/jcengi/2016/6762390/cta/

[40] A. G. Lazaropoulos, "Measurement Differences, Faults and Instabilities in Intelligent Energy Systems–Part 1: Identification of Overhead High-Voltage Broadband over Power Lines Network Topologies by Applying Topology Identification Methodology (TIM)," *Trends in Renewable Energy*, vol. 2, no. 3, pp. 85-112, Oct. 2016. [Online]. Available: http://futureenergysp.com/index.php/tre/article/view/26/32